

*Measured Solubilities and Speciations  
of Neptunium, Plutonium, and Americium  
in a Typical Groundwater (J-13)  
from the Yucca Mountain Region  
Milestone Report 3010-WBS 1.2.3.4.1.3.1*

*H. Nitsche\**  
*R. C. Gatti\**  
*E. M. Standifer\**  
*S. C. Lee\**  
*A. Müller\**  
*T. Prussin\**  
*R. S. Deinhammer\**  
*H. Maurer\**  
*K. Becroft\**  
*S. Leung\**  
*S. A. Carpenter\**

\*Lawrence Berkeley Laboratory, University of California,  
Earth Sciences Division, 1 Cyclotron Road, Mail Stop 70-A-1150,  
Berkeley, CA 94720.

**Los Alamos**  
NATIONAL LABORATORY

Los Alamos, New Mexico ~~DISTRIBUTION~~ **DISTRIBUTION** OF THIS DOCUMENT IS UNLIMITED

**MASTER**

*Sc*

## TABLE OF CONTENTS

<u>Section</u>	<u>Page</u>
LIST OF FIGURES.....	vii
LIST OF TABLES .....	xi
1. EXECUTIVE SUMMARY.....	1
2. PURPOSE AND OBJECTIVE .....	5
3. CONCEPT OF SOLUBILITY STUDIES.....	7
3.1. Oversaturation and Undersaturation .....	8
3.2. Phase Separation.....	9
3.3. Solid Phase .....	10
3.4. Determination of Oxidation States and Speciation .....	11
4. EXPERIMENTAL DETAILS.....	13
4.1. Controlled Atmosphere Glove Box.....	13
4.2. Control System for pH and Temperature .....	15
4.3. Pressure Control System.....	15
4.4. Solutions.....	15
4.5. Phase Separation.....	19
4.6. Analysis.....	20
4.7. Criteria for Steady-State Concentrations .....	20
4.8. Eh Measurements .....	21
4.9. Identification of Solids .....	21
5. RESULTS AND DISCUSSION .....	22
5.1. Neptunium.....	22
5.1.1. Solubility.....	22
5.1.2. Speciation.....	22
5.1.3. Identification of Solids .....	32
5.2. Plutonium.....	51
5.2.1. Solubility.....	51
5.2.2. Oxidation State Determination.....	51

**TABLE OF CONTENTS (continued)**

<b><u>Section</u></b>		<b><u>Page</u></b>
5.2.3. Identification of Solids .....		61
5.3. Americium .....		73
5.3.1. Solubility.....		75
5.3.2. Speciation.....		75
5.3.3. Identification of Solids .....		75
6. REFERENCES .....		87
APPENDIX A .....		92
APPENDIX B .....		102
APPENDIX C .....		112
APPENDIX D .....		125

## LIST OF FIGURES

<u>Section</u>	<u>Page</u>
Figure 1. Results for $\text{NpO}_2^+$ solubility experiments in J-13 groundwater as a function of pH and temperature.....	23
Figure 2. Solution concentrations of $^{237}\text{Np}$ in contact with precipitate obtained from supersaturation in J-13 groundwater at 25°C as a function of time.....	25
Figure 3. Solution concentrations of $^{237}\text{Np}$ in contact with precipitate obtained from supersaturation in J-13 groundwater at 60°C as a function of time.....	26
Figure 4. Solution concentrations of $^{237}\text{Np}$ in contact with precipitate obtained from supersaturation in J-13 groundwater at 90°C as a function of time.....	27
Figure 5. Near-IR absorption spectra of Np supernatant solutions at steady state formed in J-13 groundwater at 25°C.....	28
Figure 6. Near-IR absorption spectra of Np supernatant solutions at steady state formed in J-13 groundwater at 60°C.....	29
Figure 7. Near-IR absorption spectra of Np supernatant solutions at steady state formed in J-13 groundwater at 90°C.....	30
Figure 8. FTIR spectrum of Np solid phase formed at pH 7.2 and 90°C in J-13 groundwater.....	44
Figure 9. FTIR spectrum of Np solid (green phase) formed at pH 8.4 and 90°C in J-13 groundwater.....	45
Figure 10. FTIR spectrum of Np solid (tan phase) formed at pH 8.4 and 90°C in J-13 groundwater.....	46
Figure 11. FTIR spectrum of Np solid phase formed at pH 5.9 and 90°C in J-13 groundwater.....	47

**LIST OF FIGURES (continued)**

<b>Section</b>		<b>Page</b>
Figure 12.	FTIR spectrum of Np solid phase formed at pH 5.9 and 25°C in J-13 groundwater. ....	48
Figure 13.	FTIR spectrum of Np solid phase formed at pH 7.0 and 25°C in J-13 groundwater. ....	49
Figure 14.	FTIR spectrum of Np solid phase formed at pH 8.5 and 25°C in J-13 groundwater. ....	50
Figure 15.	Results for Pu <sup>4+</sup> solubility experiments in J-13 groundwater as a function of pH and temperature. ....	52
Figure 16.	Solution concentrations of <sup>239</sup> Pu in contact with precipitate obtained from supersaturation in J-13 groundwater at 25°C as a function of time ....	54
Figure 17.	Solution concentrations of <sup>239</sup> Pu in contact with precipitate obtained from supersaturation in J-13 groundwater at 60°C as a function of time. ....	55
Figure 18.	Solution concentrations of <sup>239</sup> Pu in contact with precipitate obtained from supersaturation in J-13 groundwater at 90°C as a function of time. ....	56
Figure 19.	Plutonium oxidation state distributions of the supernatant solutions at steady state for Pu <sup>4+</sup> solubility experiments in J-13 groundwater at pH 5.9 and 25°C, 60°C, and 90°C ....	58
Figure 20.	Plutonium oxidation state distributions of the supernatant solutions at steady state for Pu <sup>4+</sup> solubility experiments in J-13 groundwater at pH 7.0 and 25°C, 60°C, and 90°C ....	59

**LIST OF FIGURES (continued)**

<b>Section</b>	<b>Page</b>
Figure 21. Plutonium oxidation state distributions of the supernatant at steady state for $\text{Pu}^{4+}$ solubility experiments in J-13 groundwater at pH 8.5 and 25°C, 60°C, and 90°C.....	60
Figure 22. FTIR spectrum of Pu solid phase formed at pH 5.9 and 25°C in J-13 groundwater .....	67
Figure 23. FTIR spectrum of Pu solid phase formed at pH 7.0 and 25°C in J-13 groundwater .....	68
Figure 24. FTIR spectrum of Pu solid phase formed at pH 8.5 and 25°C in J-13 groundwater .....	69
Figure 25. FTIR spectrum of Pu solid phase formed at pH 5.9 and 90°C in J-13 groundwater .....	70
Figure 26. FTIR spectrum of Pu solid phase formed at pH 7.2 and 90°C in J-13 groundwater.....	71
Figure 27. FTIR spectrum of Pu solid phase formed at pH 8.5 and 90°C in J-13 groundwater.....	72
Figure 28. Comparison of results for $^{241}\text{Am}^{3+}/\text{Nd}^{3+}$ and $^{243}\text{Am}^{3+}$ solubility experiments in J-13 groundwater as a function of pH and temperature.....	74
Figure 29. Results for $^{241}\text{Am}^{3+}/\text{Nd}^{3+}$ solubility experiments in J-13 groundwater as a function of pH and temperature .....	76
Figure 30. Solution concentration of $^{241}\text{Am}/\text{Nd}$ in contact with precipitate obtained from supersaturation in J-13 groundwater at 25°C as a function of time .....	78

**LIST OF FIGURES (continued)**

<b>Section</b>		<b>Page</b>
Figure 31.	Solution concentration of $^{241}\text{Am}/\text{Nd}$ in contact with precipitate obtained from supersaturation in J-13 groundwater at 60°C as a function of time .....	79
Figure 32.	Solution concentration of $^{241}\text{Am}/\text{Nd}$ in contact with precipitate obtained from supersaturation in J-13 groundwater at 90°C as a function of time .....	80
Figure 33.	Solution concentration of $^{243}\text{Am}$ in contact with precipitate obtained from supersaturation in J-13 groundwater at 60°C as a function of time .....	81

**LIST OF TABLES**

<b>Section</b>		<b>Page</b>
Table I.	Summary of results for solubility experiments of neptunium in J-13 groundwater at pH 5.9, 7.0, and 8.5 and at 25°, 60°, and 90°C. ....	2
Table II.	Summary of results for solubility experiments of plutonium in J-13 groundwater at pH 5.9, 7.0, and 8.5 and at 25°, 60°, and 90°C. ....	3
Table III.	Summary of results for solubility experiments of americium in J-13 groundwater at pH 5.9, 7.0, and 8.4 and at 25°, 60°, and 90°C. ....	4
Table IV.	Well J-13 water composition.....	14
Table V.	Concentrations of carbon dioxide gas in argon necessary to maintain a total dissolved carbonate concentration of $2.81 \times 10^{-3}$ M in J-13 groundwater at different pH and temperatures .....	17
Table VI.	Comparison of steady-state solution concentrations for neptunium in J-13 groundwater at 25°, 60°, and 90°C .....	24
Table VII.	Comparison of extent of carbonate complexation for steady-state solutions of neptunium in J-13 groundwater at 25°, 60°, and 90°C .....	31
Table VIII.	X-ray powder diffraction patterns of neptunium solid phases in J-13 groundwater at 25°, 60°, and 90°C and pH 5.9.....	33
Table IX.	X-ray powder diffraction patterns of neptunium solid phases in J-13 groundwater at 25°, 60°, and 90°C and pH 7 .....	34
Table X.	X-ray powder diffraction patterns of neptunium solid phases in J-13 groundwater at 25°, 60°, and 90°C and pH 8.5.....	35

**LIST OF TABLES (continued)**

<b>Section</b>		<b>Page</b>
Table XI.	X-ray powder diffraction patterns of neptunium solid phases in J-13 groundwater at 25°, pH 5.9, pH 7.0, and pH 8.5 compared with the pattern of $\text{Na}_{0.6}\text{NpO}_2(\text{CO}_3)_{0.8}\cdot2.5\text{ H}_2\text{O}$ .....	37
Table XII.	X-ray powder diffraction patterns of neptunium solid phases in J-13 groundwater at 25°, pH 5.9, pH 7.0, and pH 8.5 compared with the pattern of $\text{Na}_{0.6}\text{NpO}_2(\text{CO}_3)_{0.8}\cdot\text{nH}_2\text{O}$ .....	38
Table XIII.	X-ray powder diffraction patterns of neptunium solid phases in J-13 groundwater at 25°, pH 5.9, pH 7.0, and pH 8.5 compared with the pattern of $\text{Na}_3\text{NpO}_2(\text{CO}_3)_2\cdot\text{nH}_2\text{O}$ .....	39
Table XIV.	X-ray powder diffraction patterns of neptunium solid phases in J-13 groundwater at 90°C, pH 5.9, and pH 7.2 compared with the pattern of $\text{Np}_2\text{O}_5$ .....	40
Table XV.	X-ray powder diffraction patterns of neptunium solid phases in J-13 groundwater at 90°C, pH 7.2 (phase 2), and pH 8.4 (green phase 3 and tan phase 4) compared with the pattern of $\text{KNpO}_2\text{CO}_3$ .....	41
Table XVI.	Comparison of steady-state solution concentrations for plutonium in J-13 groundwater at 60° and 90°C.....	53
Table XVII.	Distribution of plutonium oxidation states in J-13 groundwater solutions at steady state and various pH values and temperatures of 25°, 60° and 90°C .....	57
Table XVIII.	X-ray powder diffraction patterns of plutonium solid phases in J-13 groundwater at 25°, 60°, and 90°C and pH 5.9.....	63
Table XIX.	X-ray powder diffraction patterns of plutonium solid phases in J-13 groundwater at 25°, 60°, and 90°C and pH 7 .....	64

**LIST OF TABLES (continued)**

<b>Section</b>		<b>Page</b>
Table XX.	X-ray powder diffraction patterns of plutonium solid phases in J-13 groundwater at 25°, 60°, and 90°C and pH 8.5.....	65
Table XXI.	Comparison of steady-state solution concentrations for americium-241/neodymium and americium-243 in J-13 groundwater at 25°C, 60°C and 90°C.....	77
Table XXII.	X-ray powder diffraction patterns of $^{241}\text{Am}/\text{Nd}$ solid phases in J-13 groundwater at 25°C, 60°C, and 90°C and pH 5.9 compared with the patterns of hexagonal and orthorhombic $\text{NdOHCO}_3$ .....	82
Table XXIII.	X-ray powder diffraction patterns of $^{241}\text{Am}/\text{Nd}$ solid phases in J-13 groundwater at 25°C, 60°C, and 90°C and pH 7 compared with the pattern of orthorhombic $\text{NdOHCO}_3$ .....	83
Table XXIV.	X-ray powder diffraction patterns of $^{241}\text{Am}/\text{Nd}$ solid phases in J-13 groundwater at 25°C, 60°C, and 90°C and pH 8.5.....	84
Table XXV.	X-ray powder diffraction patterns of $^{243}\text{Am}$ solid phases in J-13 water at 60°C and pH 5.9, 7.0 and 8.5 compared with the pattern of orthorhombic $\text{NdOHCO}_3$ .....	86



**MEASURED SOLUBILITIES AND SPECIATIONS OF NEPTUNIUM,  
PLUTONIUM, AND AMERICIUM IN A TYPICAL GROUNDWATER  
(J-13) FROM THE YUCCA MOUNTAIN REGION  
MILESTONE REPORT 3010-WBS 1.2.3.4.1.3.1**

by

**H. Nitsche, R. C. Gatti, E. M. Standifer, S. C. Lee,  
A. Müller, T. Prussin, R. S. Deinhammer, H. Maurer,  
K. Becraft, S. Leung, and S. A. Carpenter**

**ABSTRACT**

**Solubility and speciation data are important in understanding aqueous radionuclide transport through the geosphere. They define the source term for transport retardation processes such as sorption and colloid formation. Solubility and speciation data are useful in verifying the validity of geochemical codes that are part of predictive transport models. Results are presented from solubility and speciation experiments of  $^{237}\text{NpO}_2^+$ ,  $^{239}\text{Pu}^{4+}$ ,  $^{241}\text{Am}^{3+}/\text{Nd}^{3+}$ , and  $^{243}\text{Am}^{3+}$  in J-13 groundwater (from the Yucca Mountain region, Nevada, which is being investigated as a potential high-level nuclear waste disposal site) at three different temperatures (25°, 60°, and 90°C) and pH values (5.9, 7.0, and 8.5). The solubility-controlling steady-state solids were identified and the speciation and/or oxidation states present in the supernatant solutions were determined. The neptunium solubility decreased with increasing temperature and pH. Plutonium concentrations decreased with increasing temperature and showed no trend with pH. The americium solutions showed no clear solubility trend with increasing temperature and increasing pH.**

## 1. EXECUTIVE SUMMARY

We studied the solubilities of neptunium, plutonium, and americium in J-13 ground-water from the Yucca Mountain region (Nevada) at three temperatures and three hydrogen ion concentrations. They are 25°, 60, and 90°C and pH 5.9, 7.0, and 8.5. Tables I, II, and III summarize the results for neptunium, plutonium, and americium, respectively. The solubilities were studied from oversaturation. The nuclides were added at the beginning of each experiment as  $\text{NpO}_2^+$ ,  $\text{Pu}^{4+}$ , and  $\text{Am}^{3+}$ .

The neptunium solubility decreased with increasing temperature and with increasing pH. The soluble neptunium did not change oxidation state at steady state. The pentavalent neptunium was increasingly complexed by carbonate with increasing pH. The steady-state solids were crystalline sodium neptunium carbonate hydrates with different water content, except the solid formed at 90°C and pH 5.9. We identified this solid as crystalline  $\text{Np}_2\text{O}_5$ . The 90°C, pH 7 solid was a mixture of sodium neptunium carbonate hydrate and neptunium pentoxide.

Plutonium concentrations decreased with increasing temperature and showed no trend with pH.  $\text{Pu(V)}$  and  $\text{Pu(VI)}$  were the dominant oxidation states in the supernatant solution; as the amount of  $\text{Pu(V)}$  increased with pH,  $\text{Pu(VI)}$  decreased. The solubility-controlling steady-state solids were mostly amorphous, although some contained a crystalline component. They contained mainly  $\text{Pu(IV)}$  polymer and smaller portions of plutonium carbonates.

For the americium solutions, no clear solubility trend was found with increasing temperature and increasing pH. Much higher solubilities were found for 60°C compared with 25°C and 90°C. All solids were  $\text{AmOHCO}_3$ , with orthorhombic structure for all temperatures at pH 7 and 8.5 and for 60°C at pH 6 and with hexagonal structure for 25°C and 90° at pH 6. Orthorhombic  $\text{AmOHCO}_3$  appears to have a much higher solubility at pH 6 and 60°C than the hexagonal form at the same pH and 25°C or 90°C.

**Table I. Summary of results for solubility experiments on neptunium in J-13 groundwater at pH 5.9, 7.0, and 8.5 and at 25°, 60°, and 90°C.**

	Steady-state concentration (M)			Oxidation state in supernatant solution		
	25°C	60°C	90°C	25°C	60°C	90°C
pH 5.9	$(5.3 \pm 0.3) \times 10^{-3}$	$(6.4 \pm 0.4) \times 10^{-3}$	$(1.2 \pm 0.1) \times 10^{-3}$	V: 100% 9% carbonate complexed	V: 100%, 8% carbonate complexed	V: 100%, uncomplexed
pH 7.0	$(1.3 \pm 0.2) \times 10^{-4}$	$(9.8 \pm 1.0) \times 10^{-4}$	$(1.5 \pm 0.4) \times 10^{-4}$	V: 100%, 54% carbonate complexed	V: 100%, 15% carbonate complexed	V: 100%, uncomplexed
pH 8.5	$(4.4 \pm 0.7) \times 10^{-5}$	$(1.0 \pm 0.1) \times 10^{-4}$	$(8.9 \pm 0.4) \times 10^{-5}$	V: 100%, 62% carbonate complexed	V: 100%, 84% carbonate complexed	V: 100%, 100% carbonate complexed

	Eh(mV) vs. NHE			Solid phase		
	25°C	60°C	90°C	25°C	60°C	90°C
pH 5.9	$588 \pm 10$	$440 \pm 10$	$392 \pm 10$	$\text{Na}_{0.6}\text{NpO}_2(\text{CO}_3)_{0.8} \cdot 2.5\text{H}_2\text{O}$	$\text{Na}_{0.6}\text{NpO}_2(\text{CO}_3)_{0.8} \cdot 2.5\text{H}_2\text{O}$	$\text{Np}_2\text{O}_5$
pH 7.0	$482 \pm 10$	$325 \pm 10$	$299 \pm 10$	$\text{NaNpO}_2(\text{CO}_3) \cdot 2\text{H}_2\text{O}$	$\text{Na}_{0.6}\text{NpO}_2(\text{CO}_3)_{0.8} \cdot 2.5\text{H}_2\text{O}$	$\text{Np}_2\text{O}_5$ and a carbonate-containing solid
pH 8.5	$497 \pm 10$	$215 \pm 10$	$159 \pm 10$	$\text{Na}_{0.6}\text{NpO}_2(\text{CO}_3)_{0.8} \cdot 2.5\text{H}_2\text{O}$	$\text{Na}_{0.6}\text{NpO}_2(\text{CO}_3)_{0.8} \cdot 2.5\text{H}_2\text{O}$	crystalline, contains carbonate, unidentified

**Table II. Summary of results for solubility experiments on plutonium in J-13 groundwater at pH 5.9, 7.0, and 8.5 and at 25°, 60°, and 90°C.**

	Steady-state concentration (M)			Oxidation state in supernatant solution		
	25°C	60°C	90°C	25°C	60°C	90°C
pH 5.9	$(1.1 \pm 0.4) \times 10^{-6}$	$(2.7 \pm 1.1) \times 10^{-8}$	$(6.2 \pm 1.9) \times 10^{-9}$	III + poly: (3 ± 1)% IV: (5 ± 1)% V: (68 ± 7)% VI: (29 ± 3)%	III + poly: (10 ± 2)% IV: (2 ± 1)% V: (17 ± 5)% VI: (72 ± 5)%	III + poly: (9 ± 5)% IV: (6 ± 5)% V: (79 ± 7)% VI: (6 ± 5)%
pH 7.0	$(2.3 \pm 1.4) \times 10^{-7}$	$(3.7 \pm 0.9) \times 10^{-8}$	$(8.8 \pm 0.8) \times 10^{-9}$	III + poly: (5 ± 1)% IV: (6 ± 1)% V: (73 ± 7)% VI: (18 ± 2)%	III + poly: (3 ± 1)% IV: (2 ± 1)% V: (44 ± 9)% VI: (52 ± 4)%	III + poly: (45 ± 2)% IV: (13 ± 1)% V: (48 ± 3)% VI: (3 ± 3)%
pH 8.5	$(2.9 \pm 0.8) \times 10^{-7}$	$(1.2 \pm 0.1) \times 10^{-7}$	$(7.3 \pm 0.4) \times 10^{-9}$	III + poly: (3 ± 1)% IV: (6 ± 1)% V: (63 ± 6)% VI: (27 ± 3)%	III + poly: (5 ± 4)% IV: (13 ± 1)% V: (58 ± 2)% VI: (24 ± 1)%	III + poly: (11 ± 2)% IV: (10 ± 2)% V: (85 ± 4)% VI: (3 ± 3)%

	Eh(mV) vs. NHE			Solid phase		
	25°C	60°C	90°C	25°C	60°C	90°C
pH 5.9	342 ± 10	451 ± 10	360 ± 10	mostly amorphous with some crystallinity, contain carbonate and Pu(IV) polymer.		
pH 7.0	126 ± 10	386 ± 10	376 ± 10			
pH 8.5	259 ± 10	241 ± 10	133 ± 10			

**Table III. Summary of results for solubility experiments on americium in J-13 groundwater at pH 5.9, 7.0, and 8.4 and at 25°, 60°, and 90°C.**

	Steady-state concentration (M)			Oxidation state in supernatant solution		
	25°C	60°C	90°C	25°C	60°C	90°C
pH 6.0	$(1.8 \pm 0.6) \times 10^{-9}$	$(2.5 \pm 0.7) \times 10^{-6}$	$(1.7 \pm 1.9) \times 10^{-9}$	III: 100%	III: 100%	NA
pH 7.0	$(1.2 \pm 0.3) \times 10^{-9}$	$(9.9 \pm 9.2) \times 10^{-9}$	$(3.1 \pm 1.7) \times 10^{-10}$	III: 100%	III: 100%	NA
pH 8.4	$(2.4 \pm 1.9) \times 10^{-9}$	$(1.2 \pm 1.3) \times 10^{-8}$	$(3.4 \pm 2.1) \times 10^{-10}$	III: 100%	III: 100%	NA

	Eh(mV) vs. NHE			Solid phase		
	25°C	60°C	90°C	25°C	60°C	90°C
pH 5.9	$331 \pm 10$	$393 \pm 10$	NA	AmOHCO <sub>3</sub> hexagonal	AmOHCO <sub>3</sub> orthorhombic	AmOHCO <sub>3</sub> hexagonal
pH 7.0	$361 \pm 10$	$385 \pm 10$	NA	AmOHCO <sub>3</sub> orthorhombic	AmOHCO <sub>3</sub> orthorhombic	AmOHCO <sub>3</sub> orthorhombic
pH 8.4	$182 \pm 10$	$343 \pm 10$	NA	AmOHCO <sub>3</sub> orthorhombic	AmOHCO <sub>3</sub> orthorhombic	AmOHCO <sub>3</sub> orthorhombic

## 2. PURPOSE AND OBJECTIVE

Yucca Mountain, Nevada, was identified for site characterization as a potential site for a repository of high-level nuclear waste. As a worst case scenario, intrusion of water into the repository must be considered for risk assessment. Water moving through the emplacement area towards the accessible environment can transport radionuclides in two ways: either as dissolved species in the water or as particulate material by the water. The Yucca Mountain Site Characterization Plan (SCP) requires "Studies to Provide the Information Required on Radionuclide Retardation by Precipitation Processes along Flow Paths to the Accessible Environment" before licensing and construction of the repository.<sup>1</sup> The purpose of this study is to supply data for calculating radionuclide transport along potential transport pathways from the repository to the accessible environment. Data derived from solubility studies are important for validating geochemical codes that are part of predictive radionuclide transport models. Such codes should be capable of predicting the results of solubility experiments. Furthermore, agreement between geochemical calculations and experimental results can validate the thermodynamic data base used with the modeling calculation.

To predict behavior at higher temperatures, data bases used for modeling calculations must contain data on thermodynamic functions at elevated temperatures. To date, many of these data are unavailable and are therefore estimated by extrapolation from lower temperature data. Agreement between modeling calculations and experimental results would also validate such estimates, whereas significant discrepancies would identify the need for data base improvement. Improvements can be made by filling the gaps with generic experimental data.

In addition, experimental solubility data also provide the source terms or the starting concentrations for experimental sorption studies. To be valid, sorption studies should be conducted at or below the solubility limit because only soluble species can be transported and participate in the sorption process.

In selecting these experiments, we have considered the generic U.S. Nuclear Regulatory Commission (NRC) technical position titled "Determination of Radionuclide Solubility in Groundwater for Assessment of High-Level Waste Isolation."<sup>2</sup> This technical position served as guidance for our experiments to determine radionuclide solubility. It requires that if radionuclide solubility is used as a factor in limiting radionuclide release, experiments must be designed to determine solubility under site-specific conditions.

Radionuclide concentrations in water passing through the emplacement area can be limited by two mechanisms: low dissolution rates of the solid waste form or solubilities of individual radionuclides. If solid waste dissolution rates are low enough, it may not be necessary to depend on solubilities to limit radionuclide concentrations. However, the solid waste forms have not yet been determined, and therefore the dissolution rates of the solid waste are unknown. Determination of radionuclide solubility limits provides an upper bound on radionuclide concentrations in solution and provides a basis for extrapolation to long-term behavior. The rate of groundwater flow through the waste is expected to be sufficiently slow to permit saturation of water with radionuclides. Dissolution limited by saturation will provide maximum concentration limits. Therefore, an assessment of radionuclide release rates using a saturation-limited dissolution model represents the most conservative approach possible.

As radionuclides are transported along flow paths to the accessible environment, changing conditions of the water (pH, Eh, oxidation state, and concentrations of complexing species) can alter solubilities. Decreases in solubility can decrease radionuclide concentrations. A knowledge of radionuclide solubilities under the conditions along possible flow paths is necessary to assess this scenario. Solubility studies are very time-consuming because long times are often needed to reach steady-state conditions. Because we cannot investigate every possible solubility scenario, we selected pH and temperature values to bracket the expected range of conditions by choosing parameters that represent lower and upper limits.

Neptunium, plutonium, and americium are expected to be sparingly soluble with solubility-limited dissolution rates. Water samples with compositions that bracket the range of waters expected in the vicinity of Yucca Mountain were chosen for solubility measurements.<sup>3</sup> These samples come from two sources. Water from Well J-13 is a reference water for the unsaturated zone near the proposed emplacement area. Well UE25p#1 taps the carbonate aquifer that underlies the emplacement horizon. This water has an ionic strength and total carbonate content higher by approximately an order of magnitude than Well J-13 water. Well J-13 water represents natural water with the highest concentrations of dissolved species expected in the vicinity of Yucca Mountain. The water from both wells is oxidizing. Generally, radionuclide solubility studies under oxidizing conditions lead to higher solubilities for a number of radionuclides than would occur under mildly or strongly reducing conditions. These experiments will therefore provide conservative results. In this study we are reporting on the results in J-13 water.

The maximum temperature of the host rock in which liquid water is present is expected to be limited by the boiling point of water at Yucca Mountain (95°C). The solubility experiments that use Well J-13 water were conducted at temperatures between 25 and 90°C. This span covers the range from pre-emplacement temperatures to the maximum temperature at which solubility would be important.

### 3. CONCEPT OF SOLUBILITY STUDIES

Solubility establishes an upper limit for the dissolved components in the source term for radionuclide migration from a repository. Studies of the solubility of radionuclides in groundwaters from a repository horizon will provide limits on their potential concentrations in those waters. Such limits are important for (1) validating an essential part of the radionuclide transport calculations and (2) providing guidance in choosing the maximum starting concentrations for radionuclide sorption experiments. Compared with multi-parameter transport models, laboratory solubility experiments are controlled by

fewer variables. If geochemical codes such as EQ3/6, are to be included in the transport model, the model should be capable of predicting the results of solubility experiments.

Complete solubility experiments should provide detailed knowledge of (1) the nature and chemical composition of the solubility-controlling solid, (2) the concentration of the components in solution, and (3) the identity and electrical charge of the species in the solution phase.

Meaningful thermodynamically defined solubility studies must satisfy four criteria: (1) attainment of equilibrium conditions, (2) determination of accurate solution concentrations, (3) attainment and identification of a well-defined solid phase, and (4) knowledge of the speciation/oxidation state of the soluble species at equilibrium.

### **3.1. Oversaturation and Undersaturation**

Ideally, solubility experiments should approach solution equilibrium from both oversaturation and undersaturation. The approach from oversaturation consists of adding an excess amount of the element in soluble form to the aqueous solution and then monitoring the precipitation of insoluble material until equilibrium is reached. The solid formed must then be isolated and characterized. The approach from undersaturation consists of dissolving a well-defined solid in an aqueous solution until equilibrium is reached. In both cases, the solution concentration is measured as a function of time until equilibrium is reached.

Kinetic processes will control the equilibration speed in solubility experiments. Some solutions equilibrate rapidly, others more slowly. It must be demonstrated that equilibrium is reached. This can be accomplished by experimentally determining (for both oversaturation and undersaturation experiments) the solution concentration as a function of time. When the concentration stays constant for several weeks, it is assumed that equilibrium has been established. Because this assumption is based on judgment, the term "steady state" instead of "equilibrium" is more precise. The U.S. Nuclear

Regulatory Commission (U.S. NRC) defines "steady state" as "the conditions where measurable changes in concentrations are not occurring over practical experimental times."<sup>2</sup> At steady state, thermodynamic forces may still change the solution composition: solids may become less soluble as they change from a higher to a lower free energy. The change may be very slow and may require very long or even infinite experimental times, which are not practical.

Despite this constraint, time-limited laboratory solubility experiments can supply valuable information. They provide good estimates on the upper limit of radionuclide concentrations in solution because the experimentally determined steady-state concentrations are higher than the equilibrium concentrations.

A reliable method of proving that a steady state has been reached is to approach equilibrium from both oversaturation and undersaturation. When these two experimental approaches independently produce equal solution concentrations, the data are considered reliable. For unknown solubility systems, one should first perform experiments approaching steady-state concentration from oversaturation and then characterize the solids. This has the advantage of not specifying the solid that controls solubility but of allowing the system under investigation to determine the solid that will precipitate. These solids should be synthesized for use in confirmation experiments that approach steady state from undersaturation. In this study we are reporting results for the oversaturation experiments.

### **3.2. Phase Separation**

The second criterion for meaningful solubility experiments is the derivation of accurate solution concentrations. This requires that phase separations must be as complete as possible. The separation of the solid from the solution often represents a significant practical problem in measuring solubility. Apparently higher or lower solubilities, compared with the steady-state values, can result from incomplete phase separation or from

sorption of solute during and after the separation. Incomplete phase separations (leaving some of the solid with the solution phase) lead to higher radionuclide solubilities. Lower solubilities are measured if constituents of the steady-state solution have been sorbed on filters during a filtration and on container walls after the separation.

Experimentally, the solids and solutions are separated on the basis of differences in size (via filtration) or density (via sedimentation or centrifugation). Filtration is the more commonly applied technique because it physically partitions the solute and solids. Ultrafiltration (i.e., filtration using membranes  $\leq 0.1 \mu\text{m}$ ) can effectively remove solids and colloidal particles from aqueous solution. A potential problem with ultrafiltration is adsorption of soluble species on ultrafiltration membranes. Effective filters for solubility studies must pass soluble species quantitatively; that is, either the filter should have no active sorption sites at all or any such sites should be irreversibly blocked. Filters are adequate if they have a small enough pore size to retain the solids and colloids and if they also show no sorption or only minimal sorption during multiple filtrations. Because adsorption of soluble radionuclide species on filters can be dependent on the solution's pH and on the solution species, it is mandatory to verify that possible sorption sites are indeed blocked. Usually the sorptive sites on a filter and filter housing are blocked by preconditioning of these materials. The filter is preconditioned by filtering a volume of the respective radionuclide solution through it and then discarding the filtrate. The volume required for preconditioning is determined experimentally. Details for this procedure are given in Section "4.5 Phase Separation."

### 3.3. Solid Phase

Solubility depends strongly on the state of the solid phase. Thermodynamically meaningful results require the existence of a well-defined solid phase, which ideally consists of crystalline material. The solids formed from the oversaturation in solubility tests must be clearly identified by physical or chemical characterization methods. Only when

identified unambiguously can the solid be synthesized for use in undersaturation solubility tests. Radionuclide solids formed in laboratory experiments and in nature are often thermodynamically ill-defined amorphous precipitates. Most amorphous solids, however, will become more crystalline with time. Freshly precipitated microcrystalline solids can also convert in time to a macrocrystalline material. Improved bonding at the lattice surface results in decreasing surface area. Thus the crystalline solid of higher free energy changes to one of lower free energy (Ostwald ripening, Ostwald step rule) and become less soluble.<sup>4,5,6,7</sup>

### **3.4. Determination of Oxidation States and Speciation**

Information on oxidation states and speciation of the radionuclides in steady-state solubility solution is important for transport models simulating migration and sorption along the flow path to the accessible environment. The charge and speciation of radionuclides will control their sorption and transportation in the geologic host. Speciation measurements identify complexes that may form between radionuclides and complexing ions present in the groundwater near the repository. The oxidation state in solution describes the charge of soluble species, and speciation describes their chemical nature. Radionuclides can have a single or several different oxidation states in solution. They can be present as simple ions or as complexes. When the ions react with one or several other solution components, they can form soluble complexes.

Oxidation states and speciation in solution are commonly determined by (1) adsorption spectrophotometry, (2) ion exchange chromatography, (3) solvent extraction, (4) coprecipitation, (5) potentiometry and (6) electrochemistry. Of these methods, only absorption spectrophotometry can provide information on speciation, while the others identify only the oxidation state in solution.

Absorption spectrophotometry in J-13 water has a detection limit of about  $10^{-4}$  M. This relatively high concentration limits the application of spectrophotometry for

speciation determination in solutions from radionuclide solubility studies because the solubilities can be several orders of magnitude below  $10^{-6}$  M. Photoacoustic Spectroscopy (PAS) provides much greater sensitivity, approaching  $10^{-8}$  to  $10^{-9}$  M.<sup>8,9,10,11,12</sup>

The methods listed above as 2 through 6 determine only the oxidation state in solution because they cannot determine species. They detect the oxidation state of ions indirectly. This process is different from absorption spectrophotometry, which detects the solution species directly. The indirect methods, however, detect very small concentrations ( $10^{-10}$  M and below), which is useful for radionuclide solubility studies. Solvent extraction and coprecipitation are often used successfully to determine the oxidation states of ions in very dilute solutions.<sup>13</sup> Ion exchange chromatography is less reliable for this purpose because the exchange resin often reduces the solution ions, which gives incorrect results for the oxidation state distribution. Electrochemical detection reduces or oxidizes the solution ions and measures the potentials of the reduction and oxidation reactions, respectively. The potential then identifies the individual ion. Electrochemistry needs fast kinetics and reversible thermodynamics for the reduction or oxidation step. These experiments greatly limit the method because many radionuclide ion redox reactions are irreversible and slow (e.g., the reactions of  $\text{NpO}_2^+/\text{Np}^{4+}$ ,  $\text{PuO}_2^+/\text{Pu}^{4+}$ ).

The oxidation state of plutonium and americium species in solution were determined by a solvent extraction and coprecipitation technique.<sup>13</sup> The neptunium solution species were determined by spectrophotometry because the solution concentration was greater than  $10^{-6}$  M.

The sensitivity of the available analytical methods for plutonium limits this part of our study. PAS is needed to determine directly the species in the supernatant solutions of the solubility experiments at submicromolar concentrations. A related activity is currently developing this capability for the YMP. Once PAS becomes available, it will be used.

#### **4. EXPERIMENTAL DETAILS**

We studied the solubilities of neptunium, plutonium, and americium at 25°, 60°, and 90°C and respective pH values of 5.9, 7.0, and 8.5. Measurements were made in an inert-atmosphere box to avoid contamination of solutions by atmospheric CO<sub>2</sub>. The solubilities were studied from oversaturation by injecting a small amount, usually between 0.5 and 1 ml, of actinide stock solution into 80 ml of groundwater obtained from Well J-13. The analysis of the water composition is listed in Table IV. The J-13 groundwater was sampled at the site by Los Alamos personnel. It was filtered at Los Alamos before it was shipped to LBL. The water's natural carbondioxide partial pressure (p<sub>CO<sub>2</sub></sub>) could not be preserved during filtration and shipping. For the experiments, however, the natural state was induced by re-equilibrating the water with CO<sub>2</sub> gas. Details of this procedure are described in paragraphs "4.3. Pressure Control System," and "4.4. Solutions." Details of the filtration are described in paragraph "4.4. Solutions." The polyethylene shipping bottle was leached with acid and distilled water prior to its use for the groundwater. The leaching removes possible trace-level contaminants that may alter the composition of the J-13 water.

##### **4.1. Controlled-Atmosphere Glove Box**

Due to the radiation hazard of the actinide elements under investigation, all experimental work was performed in glove boxes. External CO<sub>2</sub> control of the experimental solutions requires the exclusion of atmospheric CO<sub>2</sub>. To satisfy both conditions, we used a controlled-atmosphere glove box.

**Table IV. Well J-13 water composition.<sup>3</sup>**

Species	Concentration mM
Ca	0.29
Mg	0.072
Na	1.96
K	0.136
Li	0.009
Fe	0.0008
Mn	0.00002
Al	0.0010
SiO <sub>2</sub>	1.07
F <sup>-</sup>	0.11
Cl <sup>-</sup>	0.18
SO <sub>4</sub> <sup>2-</sup>	0.19
NO <sub>3</sub> <sup>-</sup>	0.16
Alkalinity	2.34 mequiv/L
Total carbonate	2.81
pH	7.0
Eh	700 mV

#### **4.2. Control System for pH and Temperature**

Because the solubilities are highly sensitive to pH and temperature changes, close control of these parameters is necessary. We designed a computer-operated control system (pH-stat) to maintain the aqueous actinide solutions at constant temperatures and pH values for the solubility experiments.<sup>14</sup> The pH-stat records and adjusts the pH values of the experimental solutions (J-13 water) at the target values with standard deviations not exceeding 0.1 pH unit. It uses small amounts (usually between 5 to 50 microliters) of dilute (0.05–0.1 M) HClO<sub>4</sub> or NaOH solution for the pH adjustments. The water chemistry was not substantially affected by this adjustment. Temperatures from 25° to 90°C were controlled within less than 1°C.

#### **4.3. Pressure Control System**

We designed and manufactured a pressure regulation system to maintain the well waters used in experiments at their nominal carbonate concentrations when their temperatures and pH values are adjusted to conditions differing from their natural state. The system also ensured that no significant evaporative loss of the solutions occurred at elevated temperatures.

#### **4.4. Solutions**

The actinide stock solutions were prepared by using established methods.<sup>15</sup> <sup>237</sup>Np(V) and <sup>243</sup>Am(III) stock solutions were prepared by dissolving their oxides in HCl. Stable neodymium(III) was used on several occasions as an analogue for americium(III). It was prepared by dissolving Nd<sub>2</sub>O<sub>3</sub> in HClO<sub>4</sub>. The solution was then spiked with purified <sup>241</sup>Am(III) tracer to enable the use of nuclear counting for the determination of the neodymium solution concentrations. Further details for these <sup>241</sup>Am/Nd mixtures are given in section 5.3. <sup>239</sup>Pu(IV) stock was prepared from plutonium metal. The actinide solutions were purified from possible metal contaminants by ion exchange

chromatography. For neptunium and plutonium, anion exchange was used, while cation exchange was employed for americium. The purity of these stock solutions was tested by spark emission spectroscopy, and no contaminants were found above the detection limits of the method. The solutions were converted to a non-complexing perchlorate system. The neptunium and plutonium stock solutions were in the oxidation state +6 after their conversion to perchlorate and were reduced electrolytically to  $\text{NpO}_2^+$  and  $\text{Pu}^{4+}$ , respectively.<sup>16,17,18</sup> Valence purity was established by absorption spectrophotometry.<sup>19,20</sup>

The groundwater, was filtered through 0.05  $\mu\text{m}$  polycarbonate membrane filters (Nuclepore Corp., Pleasanton, CA). This filtration was carried out by Los Alamos personnel prior to shipping the J-13 water sample to LBL. The actinide stock solutions, and all other solutions utilized in this experiment were filtered through 0.22  $\mu\text{m}$  polyvinylidene difluoride syringe filter units (Millipore Corp., Bedford, MA). Filtration was used to remove suspended particulate material, e.g., dust or silica, that could absorb the actinide ions to form pseudocolloids. Before the addition of actinide stock solutions to the J-13 water, a small amount of  $\text{CO}_2$ -free sodium hydroxide solution was added in order to keep the pH values at or above the desired solution pH. Letting the pH drop below the target value would necessitate addition of concentrated base to the system while the actinide ion is already present in the solution. Addition of strong base can result in unpredictable microprecipitation and formation of microcolloids.

The well water's total dissolved carbonate ( $2.81 \times 10^{-3}$  M) was preserved at each individual pH and temperature by equilibrating the solution with mixtures of  $\text{CO}_2$  in argon.<sup>3</sup> The amount of  $\text{CO}_2$  at a given pH and temperature was calculated from Henry's constant and the dissociation constants of carbonic acid from literature data.<sup>21</sup> If the value at the given ionic strength and temperature was not available, the number was derived by interpolation of adjacent values. The concentrations of the equilibration gas mixtures are given in Table V.

**Table V. Concentrations (in percent) of carbon dioxide gas in argon to maintain a total dissolved carbonate concentration of  $2.81 \times 10^{-3}$  M in J-13 groundwater at different pH and temperatures.**

	25°C	60°C	90°C
pH 5.9	6.06	9.67	18.58
pH 7.0	1.57	2.35	4.05
pH 8.5	0.0573	0.0877	0.142

The test solutions were kept in 90 ml cells that were made of either Teflon Perfluoralkoxy (TPFA) or Polyether etherketone (PEEK). The PEEK cells were for the  $^{243}\text{Am}$  experiments because PEEK is more radiation resistant than TPFA. All cells had sealed ports at the top that accommodate the permanent emplacement of a pH electrode, an opening to draw samples, and three 1/16" diameter Teflon lines for addition of acid, base, and the  $\text{CO}_2$ -argon mixture. The temperature was controlled by placing the test cells in a heated aluminum block of LBL design. The electric heater was mounted on an orbital shaker (Lab-Line Inc., Melrose Park, IL), and all solutions were shaken continuously at approximately 100 rpm. The solutions' pH values were controlled by a computer-operated pH control system (pH-stat).<sup>14</sup> The pH-stat was designed and assembled at LBL. It records and adjusts the pH values automatically over the required long periods of time with standard deviations generally not exceeding 0.1 pH unit. We could not use the pH-stat for the 90°C experiments. The combination pH electrodes (Beckman Instr. Inc., Model 39522), used at 25° and 60°C to monitor the solutions pH values, deteriorated rather rapidly when in contact with the 90°C solutions. The deterioration is mainly due to the dissolution of the Ag/AgCl layer of the reference electrode wire and also of the wire used in the pH sensing compartment itself; the solubility of AgCl increases approximately 240 times when the temperature changes from 10° to 100°C. Although the manufacturer claims the working range of these electrodes is up to 100°C, we were unable to use the electrodes continuously with the pH-stat. Therefore, we performed the pH adjustment every day by hand: the Beckman pH electrodes were removed from the individual experimental solutions after each adjustment and reintroduced for each new measurement. Before measuring the pH, the electrodes were calibrated and remained in the solutions for several hours to come to temperature equilibrium. For the americium solubility experiments, we used Ross combination electrodes (Orion). These electrodes are stable at 95°C because they have a  $\text{I}_2/2\text{I}^-$  internal reference electrode instead of a Ag/AgCl electrode. The electrolyte bridge of the Ross electrodes however,

leaked substantially more than those of the Beckman electrodes. Placing them permanently into the test solutions would have altered the composition of the J-13 water. Therefore, we also had to adjust the pH for this experiment by hand in the same manner as we did with the Beckman pH electrodes.

#### **4.5. Phase Separation**

Achievement of steady-state conditions for the solubility measurements was monitored by sampling aliquots of the solution phases and analyzing for the respective radioisotope as a function of time. We used Centricon-30 centrifugal filters (Amicon Corp., Danvers, MA) for separating the phases of the neptunium, plutonium, and americium solutions. For the separations, the centrifuge (High-speed centrifuge, Model HSC-1000, Savant Instruments Inc.) was heated with a circulating water bath to the appropriate temperature. The filters contain a YM-type membrane with a calculated pore size of 4.1 nm. To ascertain that we achieved complete phase separation and minimal adsorption on the filters during the preparation of the solution assays, we conducted a series of filtration tests.

For each solution, these tests were done at different times during the equilibration period. We used one filter per solution and filtered consecutive portions of 500  $\mu$ L solution through it. Each filtrate was acidified to minimize sorption in the filtrate-collection container and an assay was taken. Then another 500  $\mu$ L were filtered through the same filter, collected in a new container, and assayed. This is repeated until the assays show a constant concentration. The volume necessary to saturate the filter was the cumulative amount of volumes used until the assay concentration remained constant. The presaturation volume was radionuclide-dependent.

We determined and used the following preconditioning volumes: 500  $\mu$ L, 1000  $\mu$ L, and 2000  $\mu$ L for the neptunium, plutonium, and neodymium/americium solutions, respectively.

#### 4.6. Analysis

After separation of the solution and the solid phases, the two components were analyzed separately. Concentration measurements of the supernatants were made by counting liquid aliquots with a germanium low-energy counting system (LBL design). For  $^{237}\text{Np}$ ,  $^{241}\text{Am}$ , and  $^{243}\text{Am}$  the 29.38 keV, 59.54 keV, and 74.67 keV  $\gamma$ -ray lines were used, respectively. A waiting period of at least 30 days was required for the  $^{243}\text{Am}$  samples before they could be assayed because the  $^{243}\text{Am}$  was not at secular equilibrium with the  $^{239}\text{Np}$  daughter at sampling. After this time, the 74.67 keV  $\gamma$ -line was resolved from the large Compton edge of the plutonium  $K$  x-rays and the 106.13 keV  $\gamma$ -line from the  $^{239}\text{Np}$  decay.

$^{239}\text{Pu}$  was analyzed by utilizing the  $U\text{ }L$  x-rays coming from the  $\alpha$ -decay of the plutonium. Possible contributions to the  $L$  x-rays from the decays of other radionuclides, also present in small amounts, were corrected by subtraction.<sup>22</sup> In selected cases, liquid scintillation counting was also used for plutonium concentration determinations (Packard Instr. Co., Dowers Grove, Ill., model Tri-Carb 460C). The two energy windows of the counter were set to discriminate properly between possible  $\beta$ -emitting solution contaminants and the plutonium  $\alpha$ -radiation. Repeated sample counting and the observation of a constant count rate in the  $\alpha$ -window ensured no  $\beta$ -contribution to the  $\alpha$ -count.

#### 4.7 Criteria for Steady-State Concentrations

Constant concentrations over time with minimal deviation during that time span are the criteria for determining the average steady-state concentration from the individual concentration measurements.

These limits depend on the solubility of the nuclide involved and the temperature of the experiment. High solubilities yield precise concentrations within short counting times; whereas, low solubilities yield concentration with large errors, even after very long counting times. Experiments at ambient temperatures lead to very consistent

concentrations. Elevated temperatures, however, lead to greater deviations in concentration because of the difficulties involved in maintaining elevated temperature during phase separation and sample preparation.

#### **4.8. Eh Measurements**

At the end of each solubility experiment, we measured the Eh with a platinum electrode versus a Ag/AgCl/sat. NaCl reference. We cleaned the platinum electrode with 6 M HNO<sub>3</sub> before and after each measurement. Readings were stable within 30 to 60 minutes. The electrode setup was checked with "Zobell Solution" before and after each measurement.<sup>23,24</sup> We measured the Eh values to supply future chemical modeling efforts (neptunium, plutonium, and americium solubilities in J-13 water solutions) with a reference value. Without modeling, however, the Eh measurements are only of limited value, because they may represent a combination of many different redox reactions for each individual solubility solution.

#### **4.9. Identification of Solids**

The solid compounds were analyzed by x-ray powder diffraction measurements. A few micrograms of each actinide precipitate were placed in a 0.33 mm diameter quartz capillary tube, and the tube was sealed with an oxy-butane microtorch. The tube was mounted in an 11.46 cm diameter Debye-Scherrer camera and then irradiated with x-rays from a Norelco III x-ray generator (Phillips Electronics, Inc.). Copper K<sub>α</sub> radiation filtered through nickel was used. When the solids did not produce any pattern or when the pattern could not be assigned to any known compound, Fourier transform infrared-spectroscopy (FTIR) was applied. A small amount of each solid was placed between two pre-fabricated polished KBr windows, and the windows were then sealed at the rim with epoxy. Great care was taken to keep the outside of the KBr windows free of contamination. These samples were then analyzed by FTIR (Mattson Instr., Inc., Madison, WI,

model Sirius 100).

## 5. RESULTS AND DISCUSSION

### 5.1. Neptunium

#### 5.1.1. Solubility

Results of the neptunium solubility studies are shown in Figure 1. The neptunium was initially introduced as  $\text{NpO}_2^+$  into the J-13 groundwater. The steady-state concentrations and the solutions' Eh values are given in Table VI. Concentration profiles as a function of equilibration time and pH for 25°, 60°, and 90°C are shown in Figures 2, 3, and 4, respectively. The individual measurements are listed in Appendix A. At each temperature the neptunium solubility decreased with increasing pH. No significant temperature dependence was found within each individual temperature studied.

#### 5.1.2. Speciation

The supernatant solutions were analyzed by absorption spectrophotometry to determine the oxidation state and speciation. The spectra are shown in Figures 5, 6, and 7 for 25°, 60°, and 90°C, respectively. The supernatant samples from the experiments at pH 6, 25° and 60°C were diluted with J-13 water to keep the absorbance value within the sensitivity limit of the spectrophotometer used. With the exception of the spectra at 90°C and pH 6 and 7, all other spectra show the  $\text{NpO}_2^+$  main absorption band at 980 nm and an additional band at 992 nm that increases with pH due to the increasing carbonate complexation. The band at 980 nm is characteristic for uncomplexed  $\text{NpO}_2^+$ . The band at 992 nm is typical for neptunyl(V) carbonate complexation.<sup>25</sup>

From the difference between the total amount of neptunium (determined by  $\gamma$ -spectroscopy) and the free  $\text{NpO}_2^+$  (determined from the 980 nm peak), we calculated the amount of neptunium present as carbonate complex. The results for the amount of carbonate complexation in the steady-state solutions are given in Table VII. Because the

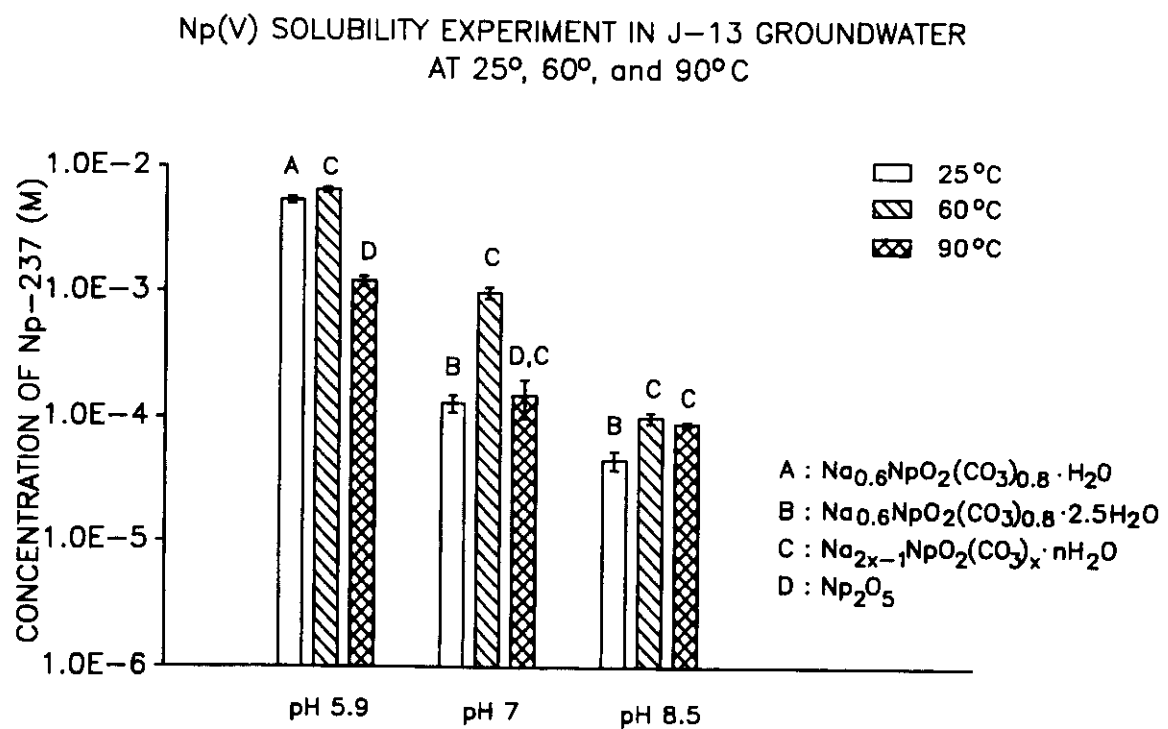


Figure 1. Results for  $\text{NpO}_2^+$  solubility experiments in J-13 groundwater as a function of pH and temperature.

**Table VI. Comparison of steady-state solution concentrations for neptunium in J-13 groundwater at 25°, 60°, and 90°C.**

25°C			
Np	pH	conc. (M)	Eh (mV vs. NHE)
	$5.9 \pm 0.1$	$(5.3 \pm 0.3) \times 10^{-3^c}$	$588 \pm 10$
	$6.9 \pm 0.1$	$(1.3 \pm 0.2) \times 10^{-4^b}$	$482 \pm 10$
	$8.5 \pm 0.1$	$(4.4 \pm 0.7) \times 10^{-5^d}$	$497 \pm 10$

60°C			
Np	pH	conc. (M)	Eh (mV vs. NHE)
	$5.9 \pm 0.1$	$(6.4 \pm 0.4) \times 10^{-3^a}$	$440 \pm 10$
	$7.1 \pm 0.1$	$(9.8 \pm 1.0) \times 10^{-4^a}$	$325 \pm 10$
	$8.5 \pm 0.1$	$(1.0 \pm 0.1) \times 10^{-4^b}$	$215 \pm 10$

90°C			
Np	pH	conc. (M)	Eh (mV vs. NHE)
	$5.9 \pm 0.2$	$(1.2 \pm 0.1) \times 10^{-3^b}$	$392 \pm 10$
	$7.2 \pm 0.2$	$(1.5 \pm 0.4) \times 10^{-4^a}$	$299 \pm 10$
	$8.4 \pm 0.1$	$(8.9 \pm 0.4) \times 10^{-5^c}$	$159 \pm 10$

(a-e): the steady-state values were determined from the last a) 5, b) 6,  
 c) 9, d) 12, e) 15 samplings.

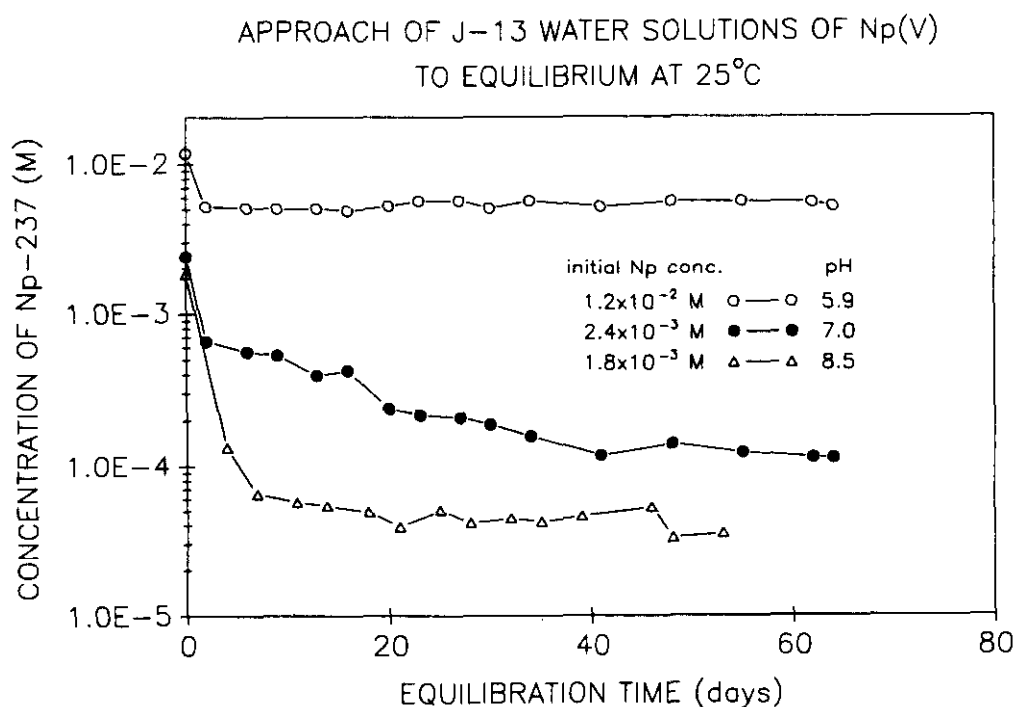


Figure 2. Solution concentrations of  $^{237}\text{Np}$  in contact with precipitate obtained from supersaturation of J-13 groundwater at 25°C as a function of time. pH  $5.9 \pm 0.1$  (open circles), pH  $6.9 \pm 0.1$  (filled circles), and pH  $8.5 \pm 0.1$  (triangles). The neptunium was added initially (day 0) as  $\text{NpO}_2^+$ ; initial concentrations were  $1.2 \times 10^{-2}$  M (pH 5.9),  $2.4 \times 10^{-3}$  M (pH 7), and  $1.8 \times 10^{-3}$  M (pH 8.5).

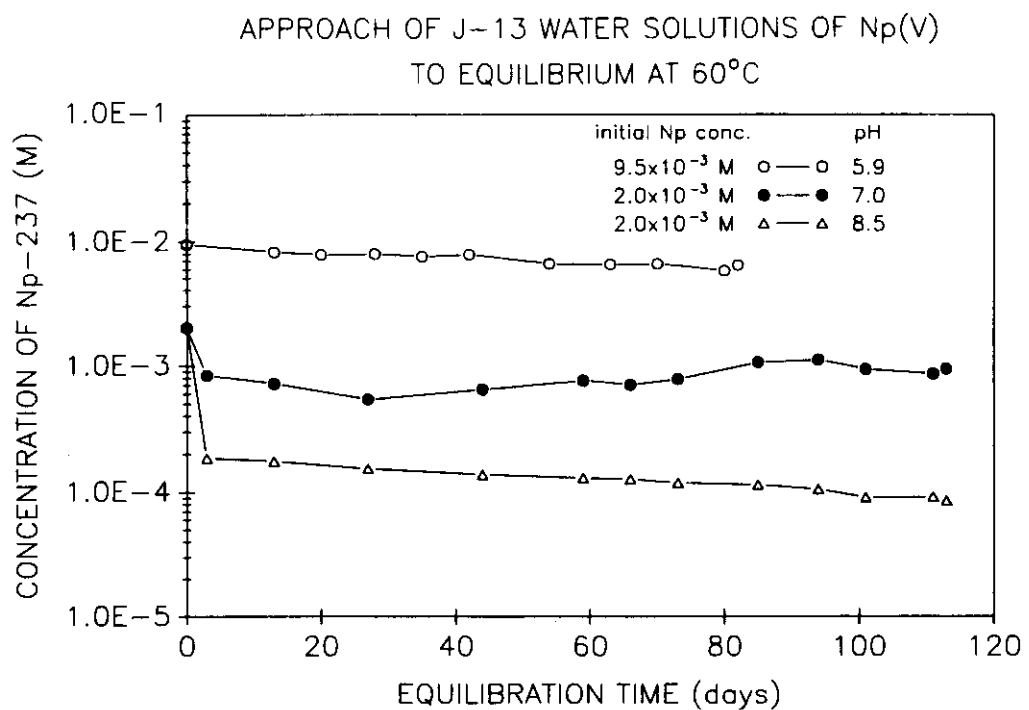


Figure 3. Solution concentrations of  $^{237}\text{Np}$  in contact with precipitate obtained from supersaturation in J-13 groundwater at 60°C as a function of time. pH  $5.9 \pm 0.1$  (open circles), pH  $7.1 \pm 0.1$  (filled circles), and pH  $8.5 \pm 0.1$  (triangles). The neptunium was added initially (day 0) as  $\text{NpO}_2^+$ ; initial concentrations were  $9.5 \times 10^{-3}$  M (pH 5.9) and  $2.0 \times 10^{-3}$  M (pH 7 and 8.5).

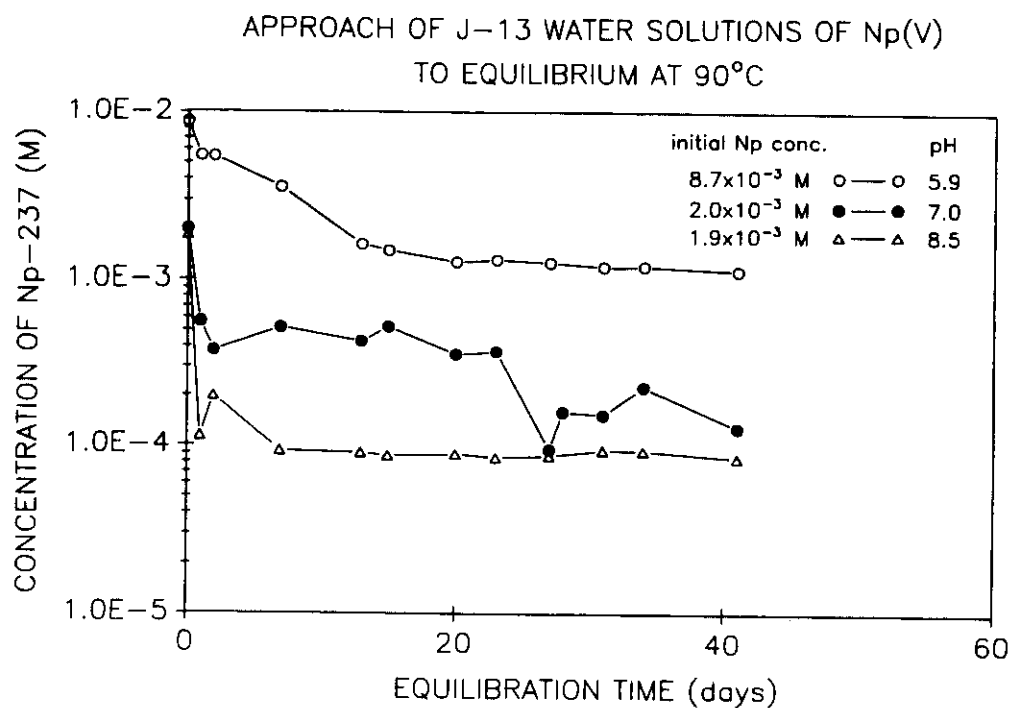
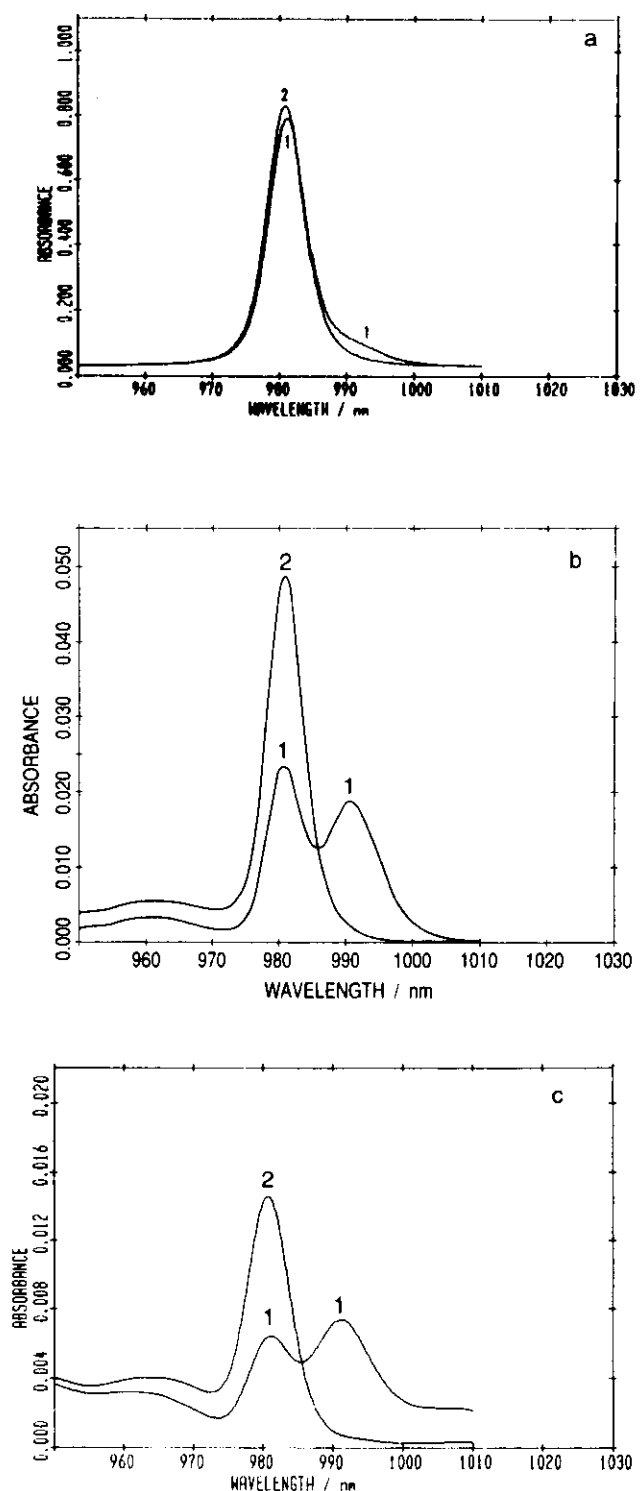


Figure 4. Solution concentrations of  $^{237}\text{Np}$  in contact with precipitate obtained from supersaturation in J-13 groundwater at 90°C as a function of time. pH  $5.9 \pm 0.2$  (open circles), pH  $7.2 \pm 0.2$  (filled circles), and pH  $8.4 \pm 0.1$  (triangles). The neptunium was added initially (day 0) as  $\text{NpO}_2^+$ ; initial concentrations were  $8.7 \times 10^{-3}$  M (pH 5.9),  $2.0 \times 10^{-3}$  M (pH 7.2), and  $1.9 \times 10^{-3}$  M (pH 8.5).



**Figure 5.** Near-IR absorption spectra of Np supernatant solutions at steady state formed in J-13 groundwater at 25°C in (a) pH 5.9, (b) pH 6.9, (c) pH 8.5: (a) at the experimental pH; (2) after acidification with HClO<sub>4</sub> to pH 0.

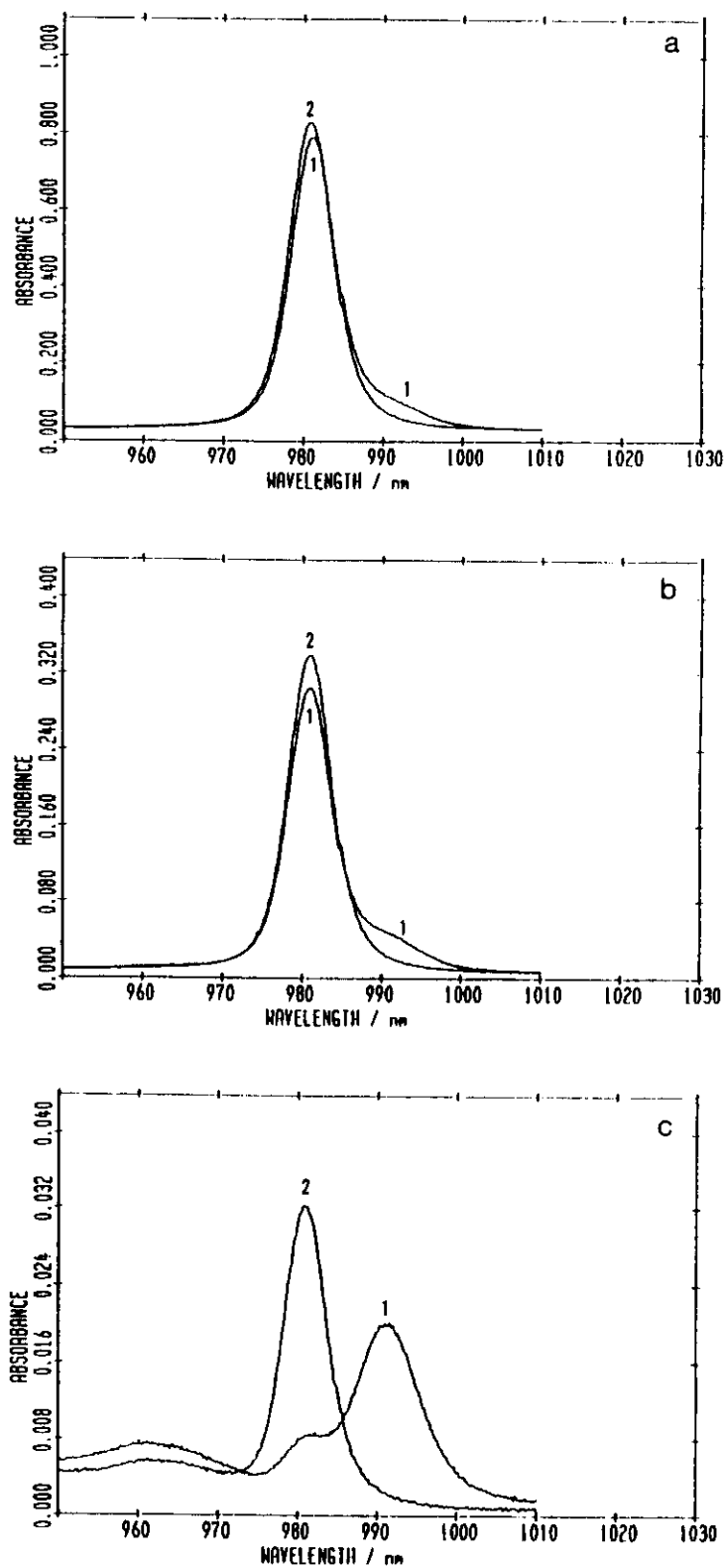


Figure 6. Near-IR absorption spectra of Np supernatant solutions at steady state formed in J-13 groundwater at 60°C in (a) pH 5.9, (b) pH 7.2, (c) pH 8.4: (1) at the experimental pH; (2) after acidification with  $\text{HClO}_4$  to pH 0.

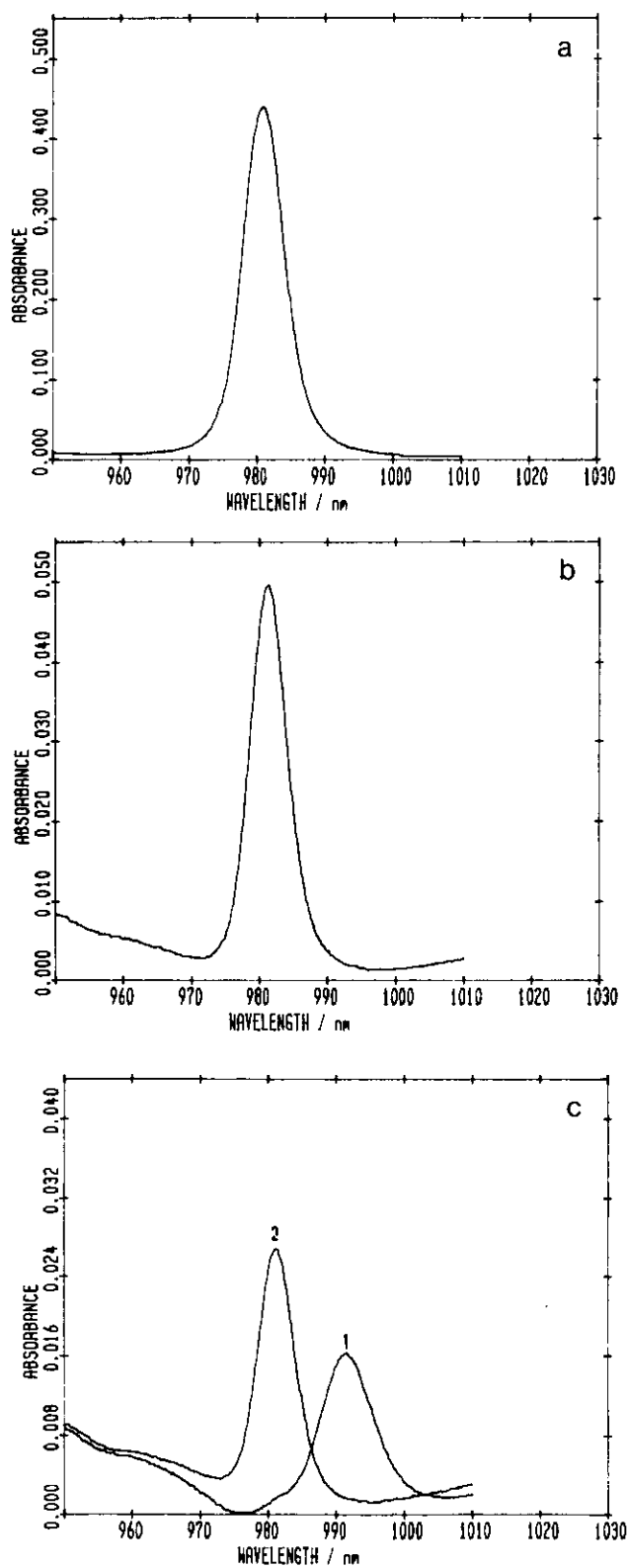


Figure 7. Near-IR absorption spectra of Np supermatant solutions at steady state formed in J-13 groundwater at 90°C in (a) pH 5.9, (b) pH 7.2, (c) pH 8.4: (1) at the experimental pH; (2) after acidification with  $\text{HClO}_4$  to pH 0.

**Table VII. Comparison of extent of carbonate complexation for steady-state solutions of neptunium in J-13 groundwater at 25°, 60°, and 90°C.**

Np Carbonate Complexation								
25°C			60°C*			90°C*		
pH	NpO <sub>2</sub> <sup>+</sup> (%)	NpO <sub>2</sub> CO <sub>3</sub> <sup>-</sup> (%)	pH	NpO <sub>2</sub> <sup>+</sup> (%)	NpO <sub>2</sub> CO <sub>3</sub> <sup>-</sup> (%)	pH	NpO <sub>2</sub> <sup>+</sup> (%)	NpO <sub>2</sub> CO <sub>3</sub> <sup>-</sup> (%)
5.9 ± 0.1	91	9	5.9 ± 0.1	92	8	5.9 ± 0.1	100	0
6.9 ± 0.1	46	54	7.1 ± 0.1	85	15	7.2 ± 0.1	100	0
8.5 ± 0.1	38	62	8.5 ± 0.1	16	84	8.4 ± 0.1	0	100

(a): distribution determined at ambient temperature